REMOVAL OF AN ANIONIC DYE FROM AQUEOUS SOLUTION BY SEPIOLITE USING A FULL FACTORIAL EXPERIMENTAL DESIGN

Özkan Demirbaş* and Mahir Alkan

University of Balikesir, Faculty of Science and Literature, Department of Chemistry, 10145 Balikesir, Turkey

ABSTRACT

Optimization of parameters by the classical batch adsorption method involves changing one independent variable and keeping the other factors constant in the same time. Classical method investigating effect of one variable at a time may be effective in some cases, but it consumes extra time and material. It requires large number of experimental trials to find out the effects. These limitations of the classical method can be eliminated by optimizing all the affecting parameters collectively by statistical experimental design. The statistical design experiments, designed to reduce the total number of experiments required, indicated that, within the selected conditions, all the parameters influenced at a significance level of 5%. In this study, batch adsorption experiments were carried out in order to evaluate the maximum adsorption conditions of the anionic dye reactive blue 220 (RB220) from aqueous solutions on sepiolite using a 2^3 full factorial design. The three factors were temperature, pH, and the ionic strength of the suspension. The optimization of the factors to obtain maximum adsorption was carried out by incorporating effect plots, normal probability plots, interaction plots, analysis of variance (ANOVA), Pareto charts, surface plots, and contour plots.

KEYWORDS: reactive dye, full factorial, statistical design, sepiolite, adsorption

1. INTRODUCTION

Dyes (over 7×10^5 metric tons of synthetic dyes) are produced worldwide every year for dyeing and printing purposes and about 5–10% of this quantity is discharged with wastewater. The amount of dye loss depends on the class of dye applied; it varies from 2% loss while using basic dyes to about 50% loss in certain reactive sulfonated dyes [1]. Reactive dyes are representing 20–30% of the total dye market and the most widely used dyes are used in the textile industry [2]. Reactive dyes are anionic dyes that depend on a negative ion [3]. Anionic dyes include many compounds from the most varied classes of dyes, which exhibit characteristic differences in structure (e.g., azoic, anthraquinone, triphenylmethan and nitro dyes) but possess a common feature, water-solubilizing, ionic substituents. The anionic dyes also include direct dyes, and from the chemical standpoint the group of anionic azo dyes includes a large proportion of the reactive dyes [4]. Most of the reactive dyes include a reactive group and interact with cotton, wool, etc., to form covalent bonds. The release of reactive dyes into the environment is undesirable, because many reactive dyes are toxic to some organisms and may cause direct destruction of creatures in water. Because of their complex structures and high solubility in water, the treatment of these pollutants particularly reactive dyes, in wastewater is troublesome [5].

Many studies have been performed to find alternative sorbents particularly for the sorption of reactive dyes from aqueous solution such as clinoptilolite [6], activated carbon [2,7,8], palygorskite [9], cationic polymer-loaded bentonite [10], peanut hull [11], pillared clays [12], natural untreated clay [13], bone char, peat and bamboo [14]. In addition, many researchers have studied the adsorption of anionic dyes using different adsorbents: organo-bentonite for the removal of Acid scarlet, Acid turquoise blue and Indigo carmine [15], ammonium-functionalized MCM-41 (a member of the mesoporous molecular sieves M41S family) for Reactive brilliant red, Acid fuchsine, Orange IV and Methyl orange [16], apatitic tricalcium phosphate and apatitic octocalcium phosphate for Reactive Yellow 4 (RY4) [17], wood-shaving bottom ash for Red reactive 141 [18], sepiolite for Brilliant yellow [19], pine cone for Acid black 26, Acid green 25 and Acid blue 7 [20] and bagasse ash for Acid blue 80 [21]. In the last few years agricultural solid wastes (mango seed [22], soy meal [23], bagasse [24] and bamboo [25]) have been used intensely as low-cost, available adsorbents for the adsorption of anionic dyes.

Sepiolite is an oxide mineral with a unit cell formula $Si_{12}O_{30}Mg_8(OH,F)_4(H_2O)_4.8H_2O$ [26]. In some aspects se-

* Corresponding author

piolite is similar to other 2:1 trioctahedral silicates, such as talc (molecule formula $Mg_3Si_4O_{10}(OH)_2$) [27, 28]. Sepiolites, which form an important group of clay minerals, are a magnesium silicate and currently used in a number of different applications such as many industrial, catalytic and environmental applications, most of which are similar to those of the more traditional clays. Because of their structural morphology, sepiolites have received considerable attention with regard to the adsorption of organics on the clay surfaces and to their use as support for catalysts [29]. The abundance and availability of sepiolite mineral reserves as a raw material source and its relatively low cost guarantee its continued utilization in the future.

Optimization of parameters by the classical method involves changing one independent variable and keeping the other factors constant in the same time. This method investigating effect of one variable at a time may be effective in some cases, but it consumes extra time and material. It requires large number of experimental trials to find out the effects. Also, this method is unreliable and fails to consider the combined effects of all the factors involved. The limitations of the conventional method can be eliminated by optimizing all the affecting parameters collectively by statistical experimental design. Optimization of parameters of a process is usually carried out by factorial, or more commonly fractional factorial, design of experiment (DOE) [30]. When the number of factors for studying is large, the factors are first screened using two level DOEs, which allow to study the effect of a large number of factors [31]. When using such methodologies, significant and more important factors are identified. In addition, some workers used different methodology and design for the adsorption processes. For example Khalili and Bonakdarpour [32] showed the statistical analysis of the results of Plackett–Burman DOE for the anaerobic decolorization of Reactive Black 5 (RB5) by activated sludge. Khataee et al. [33] investigated the biological decolorization of a dye solution containing malachite green (MG) in the presence of macroalgae *Chara sp.* using central composite design (CCD), Das and Das [34] studied the optimization of the biosorption of Ag(I) by the macrofungus *Pleurotus platypus* using the three-level Box–Behnken factorial design [34]. Turan et al. [35] studied the adsorption of copper and zinc ions on illite and determined optimal conditions using a full factorial design [35]. Some other workers have used the response surface methodology (RSM) [36-38], Box-Behnken design [39] and central composite design [33, 40]. In this study, sepiolite was chosen for the purpose of investigating its adsorption properties for RB220 dye in aqueous solutions. A 2^3 full factorial design was used to evaluate the importance of temperature, pH and ionic strength of the suspension on the adsorption with Minitab® 16.0 software for Windows™.

2. MATERIALS AND METHODS

2.1. Materials

Reactive Blue 220 (RB220) was obtained from Setas and Eksoy Textile Co. (Bursa, Turkey). The molecular structure of RB220 used is shown in Fig. 1. The sepiolite used was obtained from Aktaş¸ Lületaşı–Eskişehir regions of Anatolia (Turkey). Sepiolite sample was treated before using in the experiments as follows [41]: The aqueous suspension containing 10 g/L sepiolite was mechanically stirred for 24 h, after waiting for about 2 min the supernatant suspension was filtered through filter paper. The solid sample was dried at 105^0C for 24 h, ground then sieved. The chemical composition of this clay obtained by X-ray florescence (XRF) is given in Table 1. The cation exchange capacity (CEC) of the sepiolite used was determined by ammonium acetate method, the density and the specific surface area by BET N_2 adsorption by Micromeritics Flow Sorb II-2300 and, the isoelectric pH of 3% aqueous suspension by Zeta Meter 3+ equipment and the other physicochemical parameters, obtained are summarised in Table 2. All chemicals were obtained from Merck and Aldrich, and were of analytical grade. All water used was of Milli-Q quality or doubly distilled.

2.2. Experimental procedure

The adsorption of the dye from aqueous solutions was performed by batch experiments in volume and concentration of the dye in the initial solution and adsorbent mass were kept constant at 100 mL of 3.0×10^{-5} M and 0.50 g. All of the dye solution was prepared with ultra pure water. Agitation was made for 2 h., which is more than sufficient time to reach equilibrium at a constant

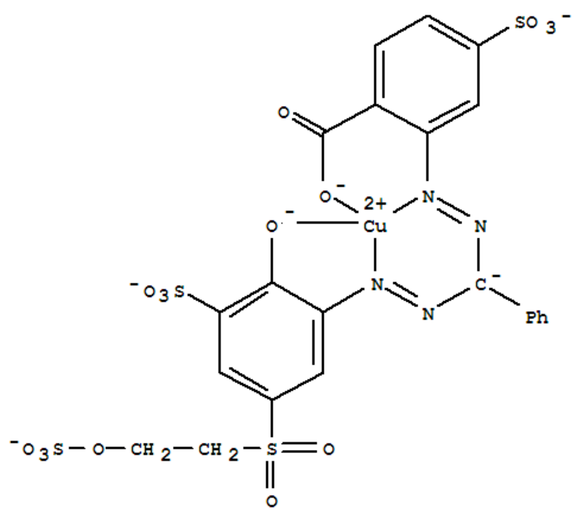

FIGURE 1 - Structure of RB220 dye

TABLE 1 - Chemical composition of sepiolite

Constituent	Percentage present
SiO_2	55.60

MgO	22.33
Al_2O_3	0.81
NiO	0.40
CaO	0.22
Fe_2O_3	0.50
Na_2O	0.11
K_2O	0.17
LoI	16.86

TABLE 2 - Some physicochemical properties of sepiolite used in this study

CEC (meq/100 g)	Particle diameter (μm)	pH of 3% aqueous solution	Density (g mL^{-1})	Specific surface area (m^2 g^{-1})	Isoelectric pH of 3% aqueous suspension	Colour
22.2	-75.0	7.7-8.5	2.43	367	6.6	White

agitation speed of 400 rpm. The pH was adjusted using 0.1N NaOH and 0.1N HCl solutions by using an Orion 920A pH-meter with a combined pH electrode. pH-meter was standardized with NBS buffers before every measurement. After 2 h, the samples were then centrifuged for 15 min at 5000 rpm and the left out concentration in the supernatant solution were analyzed using UV–Vis. spectrophotometer (Cary 1E UV–Vis. spectrophotometer, Varian) by monitoring the absorbance changes at a wavelength of maximum absorbance (600 nm). Calibration curves were plotted between absorbance and concentration of the dye solution. The adsorbent amounts q_m were calculated from the concentrations differences. The effect of pH was studied between pH 3 and 9. The adsorption studies were also carried out at 25 and 45 °C. The effect of ionic strength was studied using 0.0 and 0.1 M NaCl.

2.3. The full factorial design

The high and low levels defined for the 2^3 full factorial design are listed in Table 3. The low and high levels for the factors were selected according to some preliminary experiments. The factorial design matrix and q_m measured in each factorial experiment is shown in Table 4, with the low (−1) and high (+1) levels as specified in Table 3. q_m was determined as average of three parallel experiments. The order in which the experiments were made was randomized to avoid systematic errors. Fig. 2 illustrates the mean of the experimental results for the respective low and high levels of temperature, initial pH, and ionic strength of suspension.

TABLE 3 - The high and low levels of experimental factors.

Factor	Low level (-1)	High level (+1)
Temperature, ^0C (**A**)	25	45
pH of the dispersion (**B**)	3.0	9.0
Ionic strength of the suspension, *mol* L^{-1} (**C**)	0	0.1

TABLE 4 - Experimental design matrix and results

	Factor			q_m (mg/g)			
Run no.	A	B	C	Trial 1	Trial 2	Trial 3	Average
1	-1	-1	-1	3.507	3.518	3.508	3.511
2	-1	-1	+1	4.111	4.121	4.101	4.111
3	-1	+1	-1	3.890	3.951	3.829	3.89
4	-1	+1	+1	4.550	4.592	4.508	4.55
5	+1	+1	-1	5.151	5.148	5.154	5.151
6	+1	-1	-1	3.752	3.719	3.785	3.752
7	+1	+1	+1	4.648	4.655	4.641	4.648
8	+1	-1	+1	4.197	4.182	4.212	4.197

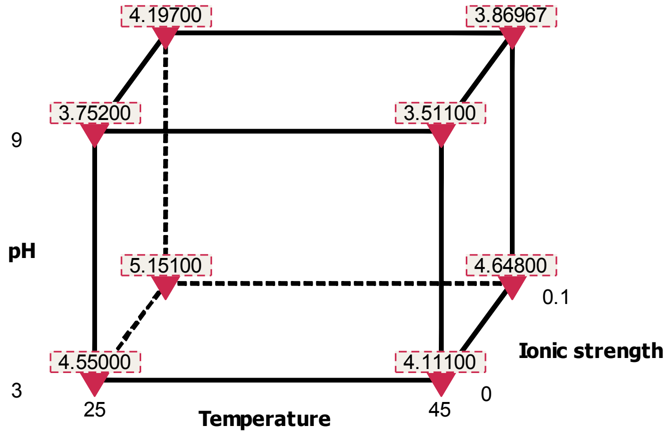

FIGURE 2 - Cube plots for q_m

3. RESULTS AND DISCUSSION

Factors that influence the adsorbed quantity of dye adsorbed onto sepiolite were evaluated by using factorial plots: main effect, interaction effect, the Pareto chart plot, normal probability plots, the surface plot, and the contour plot. ANOVA and *P*-value significant levels were used to check the significance of the effect on q_m. The main effect and interactions were also observed in the Pareto chart plot.

3.1. ANOVA

The results are displayed in Tables 5 and 6. Main, interaction effect, coefficients of the model, standard deviation of each coefficient, and probability for the full 2^3 factorial designs are presented in Table 6. The significance of the regression coefficients was determined by applying a Student's t-test. With the exception of ABC (*P*-value = 0.573), all other effects were significant with 95% confidence level. In addition, the model presented an adjusted square correlation coefficient R^2 (adj) of 99.79%, fitting the statistical model quite well. In this way, the dye uptake by sepiolite could be expressed using equation (1).

This function describes how the experimental variables and their interactions influence the dye adsorption [42]. The initial pH of the solution (B) had the greatest effect on q_m, followed by ionic strength (C), temperature (A), temperature–pH interaction (AB), pH – ionic strength interaction (BC), and temperature–ionic strength interaction (AC). The positive values of these effects reveal that the increase of these parameters increased q_m. Conversely, negative values of the effects decreased the response (q_m). According to Eq. (1), the temperature and pH had a negative effect on q_m, while ionic strength of the dispersion had a positive effect. In order to ensure an appropriate model, the test for the significance of regression was performed by applying a variance analysis (ANOVA). According to the ANOVA table, *P*-value<0.05 for the main factors and their 2-way interactions, and the R^2 value for q_m was 0.99, which was a desirable figure. Table 6 shows the sum of squares being used to estimate the factors' effect and the *F*-ratios, which are defined as the ratio of the respective mean-square-effect to the mean-square-error. The significance of these effects was evaluated using the *t*-test, and had a significance level of 5%; i.e., with a confidence level of 95%. The R-squared statistic indicated that the first-order model explained 99.85% of q_m's variability. The results revealed that the studied factors (A, B and C) and their 2-way interaction (AB, AC, and BC) were statistically significant to q_m. Notably, 3-way interaction (ABC) had no effect at the 95% confidence level.

$$q_m = 4.22 - 0.19A - 0.39B + 0.24C + 0.047AB - 0.019AC - 0.042BC \quad (1)$$

TABLE 5 -.Estimated effects and coefficients for q_m (mg/g).

Term	Effect	Coefficient	Standard error of coefficient	*T*-value	*P*-value
Constant		4.2237	0.004848	871.16	0.000
T	-0.3776	-0.1888	0.004848	-38.94	0.000
pH	-0.7826	-0.3913	0.004848	-80.71	0.000
I	0.4854	0.2427	0.004848	50.06	0.000
T*pH	0.0934	0.0467	0.004848	9.63	0.000
T*I	-0.0376	-0.0188	0.004848	-3.88	0.001
pH*I	-0.0836	-0.0418	0.004848	-8.62	0.000
T*pH*I	-0.0056	-0.0028	0.004848	-0.58	0.573
	S = 0.023752	R-Sq = 99.85%	R-Sq(pred) = 99.66%	R-Sq(adj) = 99.79%	

TABLE 6 - Analysis of variance for q_m (mg/g).

Source		Degrees of freedom	Sum of squares	Adj. Sum of squares	Adj.Mean squares	*F*-ratio	*P*-value
Main Effects		3	5.94381	5.94381	1.98127	3511.85	0.000
	A	1	0.85542	0.85542	0.85542	1516.25	0.000
	B	1	3.67462	3.67462	3.67462	6513.36	0.000
	C	1	1.41378	1.41378	1.41378	2505.95	0.000
2-Way Interactions		3	0.10275	0.10275	0.03425	60.71	0.000
	AB	1	0.05236	0.05236	0.05236	92.81	0.000
	AC	1	0.00848	0.00848	0.00848	15.02	0.001
	BC	1	0.04192	0.04192	0.04192	74.30	0.000
3-Way Interactions		1	0.00019	0.00019	0.00019	0.33	0.573
	ABC	1	0.00019	0.00019	0.00019	0.33	0.573
Residual Error		16	0.00903	0.00903	0.00056		
Pure Error		16	0.00903	0.00903	0.00056		
Total		23	6.05578				

3.2. The main effects

The main effects of each parameter on the dye adsorption are shown in Fig. 3. The main effect plots were generated to represent the results of the regression analysis. It shows only the factors that were significant at the 95% confidence interval. The main effects represent deviations of the average between the high and low levels for each factor. When the effect of a factor is positive, q_m increases as the factor changes from low to high levels. In contrast, if the effects are negative, a reduction in (q_m) occurs for high level of the same factor. From Fig. 3, it is inferred that the larger the vertical line, the larger the change in q_m when changing from level −1 to level +1. It should be pointed out that the statistical significance of a factor is directly related to the length of the vertical line [43]. The effects of temperature and pH factors are negative, that is, a decrease of q_m is observed when the factor changes from low to high. Temperature and pH factors result in a higher mean q_m at their low level, compared to that at the high level. For the ionic strength factor, the opposite is true. In addition, pH had a greater effect on q_m, as is evident by the longer vertical line. Maximum adsorption occurred at acidic pH. Fig. 3 demonstrates that the adsorption increases with decreasing pH because of the electrostatic attraction between the chromophore groups of dye and the positively charged sepiolite surface. The higher adsorption of RB220 on sepiolite at low pH may result due to the neutralization of the positive sites at the surface of sepiolite. Generally, the adsorption capacity increases with increasing pH for cationic dyes, while it decreases with increasing pH for anionic dyes [41]. We had previously shown that sepiolite had a isoelectrical point at pH 6.6 and exhibited positive zeta potential values at the lower pH values from pH 6.6, and negative zeta potential values at the higher pH values from pH 6.6 [44]. As the pH increases from 3 to 9, the number of ionisable sites on sepiolite increases. In this case:

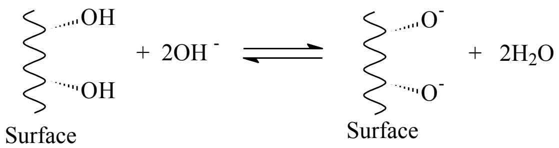

(2)

With the gradual increase in the pH of the solution, a decrease in the positive charge on the oxide or at solution interface has been observed and the adsorbent surface appears negatively charged due to deprotonation of the adsorbent surface [45]. At pH above isoelectrical point at approximately 6.6, the adsorption of the anionic dye is not favored due to electrostatic repulsion. At lower pH (pH 3), the surface of sepiolite particles may become positively charged, which enhances the negatively charged RB220 anions through electrostatic interactions. In this case, it can be written as follows:

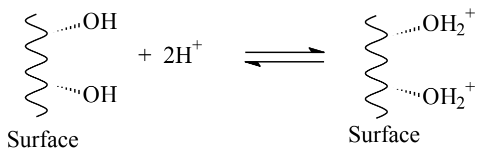

(3)

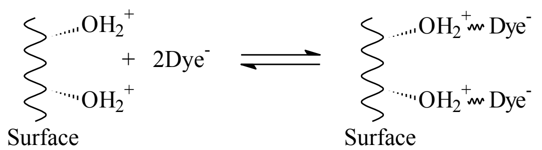

(4)

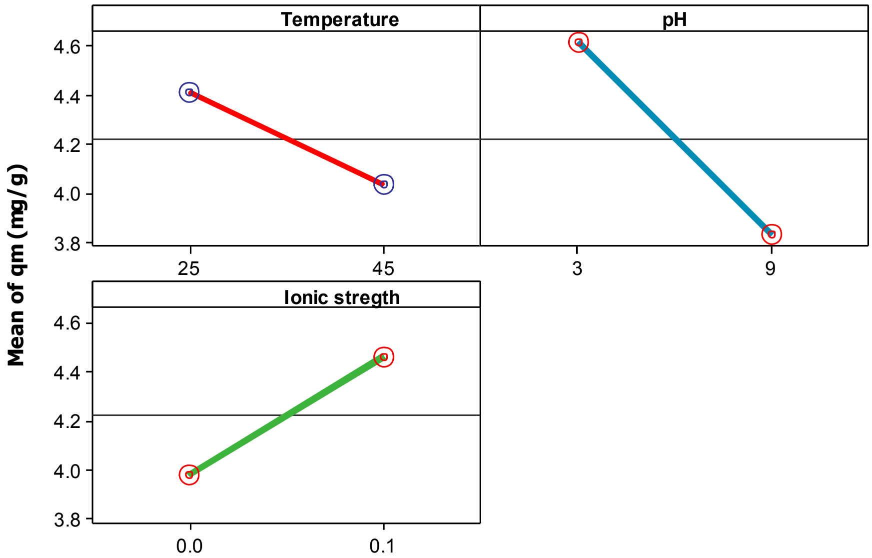

FIGURE 3 - Main effects plot for q_m.

The positively charged sites favour the adsorption of dye anionss due to electrostatic interactions [45]. A similar effect was previously reported by Alkan et al., [45, 46] for acid red 57 reactive blue 221 and acid blue 62 adsorption on sepiolite. q_m decreases as temperature increases due to the weakening of adsorptive forces between the active sites of the adsorbents and adsorbate. q_m increased with increasing ionic strength. The cause is that increasing the ionic strength increases the positive charge of the surface below the isoelectrical point, resulting in a higher attraction of anions, and increases the negative charge of the surface above isoelectrical point, increasing the repulsion of anions [45, 46].

3.3. The interaction effects

An interaction (Fig. 4) is effective when the change in the response from low to high levels of a factor is dependent on the level of a second factor, i.e. when the lines do not run parallel [47]. The interaction effect plots showed that interaction of pH, ionic strength and temperature played major role in removal. Fig. 5 shows the significant interactions between the parameters (AB, AC, and BC). The interaction plots were also generated with ANOVA. All the interactions of the factors were statistically significant in determining q_m. These plots clearly indicated that interaction between temperature and pH (AB) was stronger than between pH and ionic strength (BC). The interaction between temperature and ionic strength (AC) was statistically significant but much smaller. The effect of pH and ionic strength was more significant at lower temperatures. The interaction effects between the factors AB, AC, and BC revealed that the amount adsorbed was higher at lower temperature (A), initial pH (B) and ionic strength of the suspension (C).

3.4. The Pareto chart

The relative importance of the main effects and their interactions was also observed on the Pareto chart (Fig. 5). For the 95% confidence level, the t-value is 2.12. As shown in Fig. 5, some values are positioned around a reference line. According to Fig. 5, the main factors (A, B, and C) and their interactions (AB, AC, and BC) that extend beyond the reference line were significant at the level of 0.05. The pH represented the most significant effect on q_m. The pH (B), ionic strength interaction (C), and temperature (A) had greater effects on q_m while, except for the interaction effect between temperature, pH, and ionic strength (ABC) all other factors and their interactions had smaller effects and were statistically significant at 95% confidence.

3.5. Normal probability plots

The normal probability plot is given in Fig. 6. According to the normal probability plots, the points which are close to a line fitted to the middle group of points represent those estimated factors that do not demonstrate any significant effect on the response variables. The main factors (A, B, and C) and their interactions (AB, AC, and BC) are far away from the straight line. Because A, B, BC, and AC lie to the left of the line, their contribution had a negative effect, C and AB on the right had a positive effect. The pH (B) had largest effect because its point lies farthest from the line. These results confirm the previous Pareto chart analysis and the values of Table 5. The normal probability plot of residuals for q_m (Fig. 7) showed how closely the set of observed values followed the theoretical distribution. Generally, experimental points are reasonably aligned, suggesting a normal distribution. The selected model adequately described the observed data, explaining approximately 99% (due to R^2=0.99) of the variability of q_m.

3.6. Response surface and contour plots

The surface plots of the response functions are useful in understanding both the main and interaction effects of the factors [48]. The response surface plots are reported in Fig. 8 for the average q_m, Fig. 9 illustrates the response

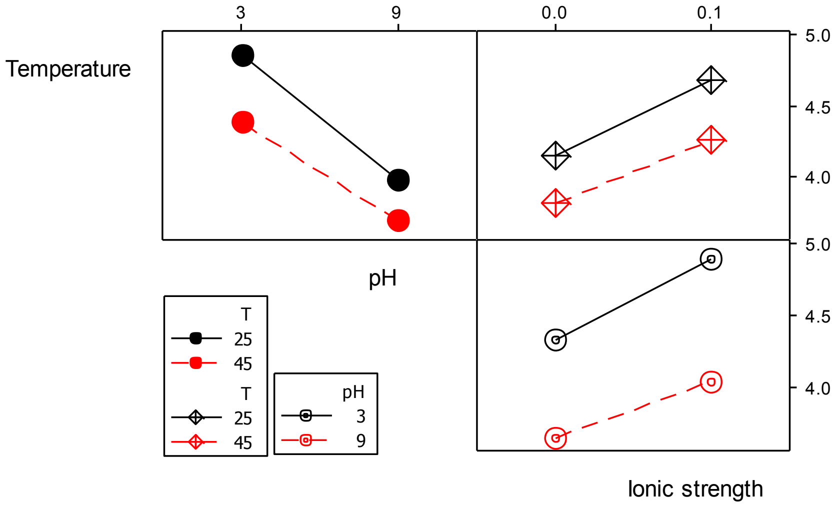

FIGURE 4 - Interaction plots for q_m

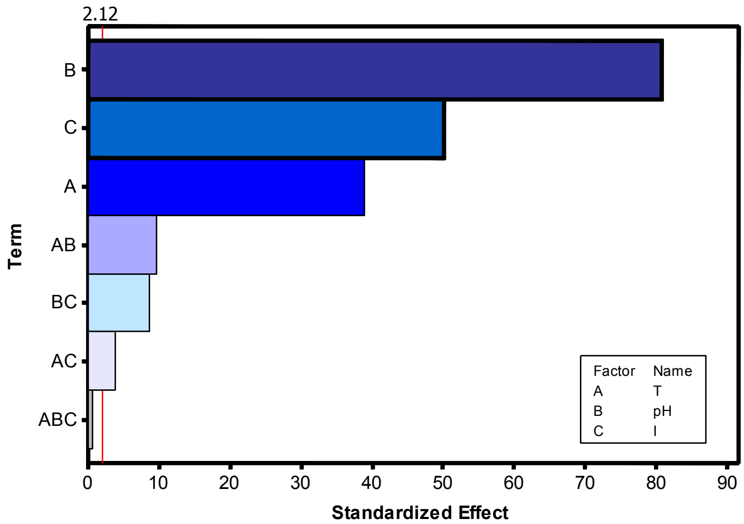

FIGURE 5 - Pareto chart of the standardized effects (Alpha = .05)

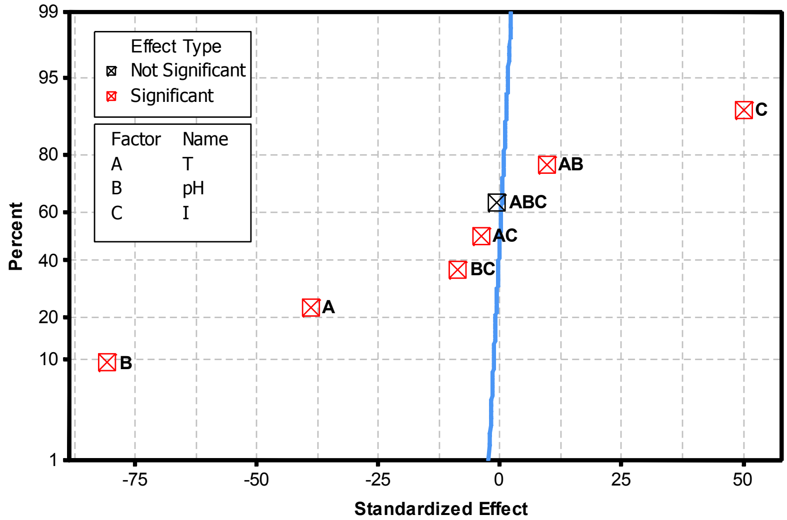

FIGURE 6 - Normal probability plot of the standardized effects (Alpha = .05)

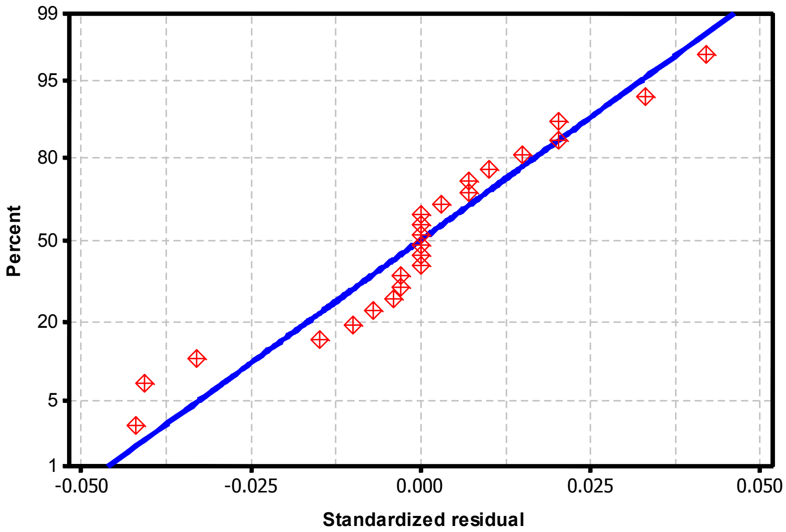

FIGURE 7- Normal probability plot of standardized residuals.

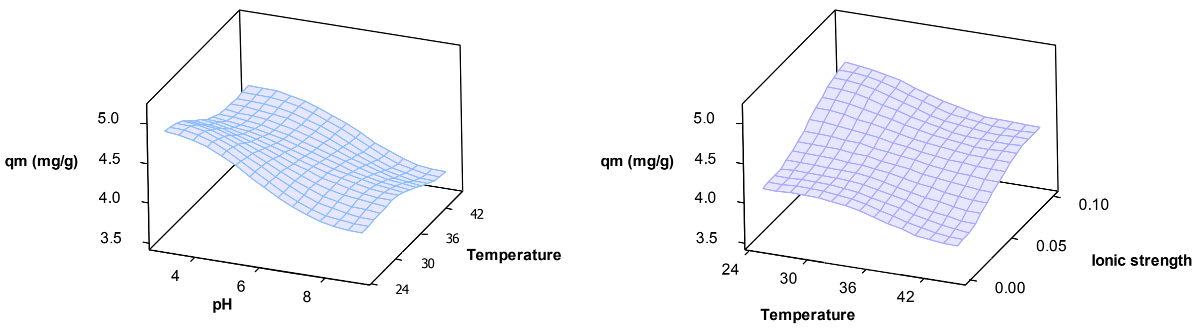

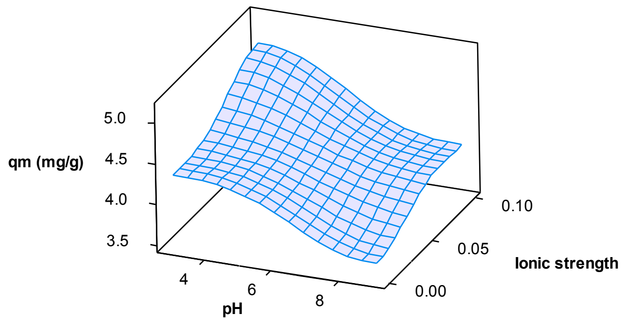

FIGURE 8 - Surface plots of q_m

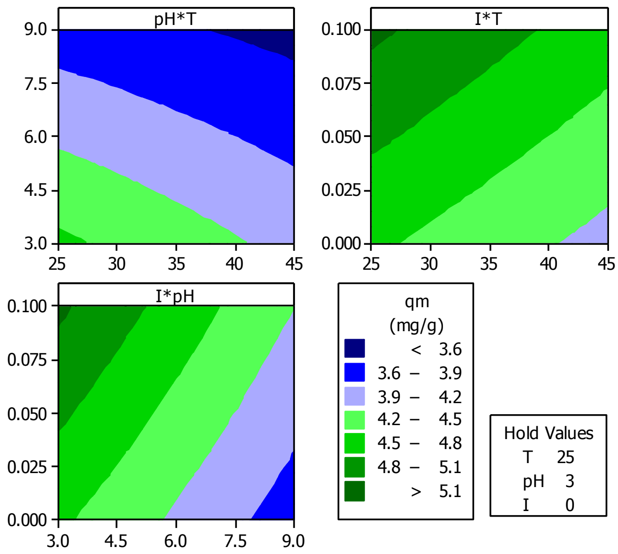

FIGURE 9 - Contour of the estimated response surface for q_m

surface counter plots when one parameter for each graph is at a hold value. This figure also shows the estimated q_m parameter as a function of the normalized independent variables, the height of the surface represents the value of q_m. From three surface plots, maximum values of q_m required lower temperature (A), pH (B), and higher ionic strength of the suspension (C) in agreement with the interaction graphs.

4. CONCLUSIONS

The following conclusions can be drawn from this investigation:

The statistical design of the experiments combined with techniques of regression was applied in optimizing the conditions of maximum adsorption of the dye onto sepiolite. Using a full factorial and laboratory scale experiment, significant process factors influencing adsorption were identified and the interactions between factors were highlighted. Three adsorption parameters (pH, temperature and ionic strength) were tested by using full factorial design criterion and all of them showed a significant effect on adsorption process. This mathematical model was used to develop contour plots for various factors' effects. It was observed that the initial pH of the suspension exerted the greatest influence on the amounts of dye adsorbed q_m. Ionic strength had positive effect but temperature and pH had a negative influence on q_m, is the validity of this study was limited to temperatures between 25 and 45 °C, pH between 3 and 9, and ionic strength of less than 0.1 M NaCl. The interactions between pH, temperature and ionic strength showed significant effect on adsorption process. Technologies for the removal of dyes are generally expensive. Thus, it may be conducted that sepiolite may be used for remove of RB220 from wastewater since it is a low-cost, abundant and locally available adsorbent in Turkey.

The authors have declared no conflict of interest.

REFERENCES

[1] Dafale, N., Rao, N.N., Meshram, S.U., Wate, S.R. (2008) Decolorization of azo dyes and simulated dye bath wastewater using acclimatized microbial consortium – biostimulation and halo tolerance. Bioresour. Technol. 99, 2552–2558.

[2] Al-Degs, Y.S., El-Barghouthi, M.I., El-Sheikh, A.H. Walker, G.A. (2008) Effect of solution pH, ionic strength, and temperature on adsorption behavior of reactive dyes on activated carbon. Dyes Pigm. 77, 16–23.

[3] Tyagi, O.D., Yadav, M.S., Yadav, M. (2002) A Textbook of Synthetic Dyes. 67, Anmol-PVT. LTD.

[4] Hunger, K. (2003) Industrial Dyes, Chemistry, Properties, Applications. Wiley-VCH, Weinheim, Germany, pp. 1–10.

[5] Y.J. Xue, H.B. Hou, S.J. Zhu (2009) Adsorption removal of reactive dyes from aqueous solution by modified basic oxygen furnace slag: isotherm and kinetic study. Chem. Eng. J. 147, 272–279.

[6] Sismanoglu, T., Kismir, Y., Karakus, S. (2010) Single and binary adsorption of reactive dyes from aqueous solutions onto clinoptilolite. J. Hazard. Mater. 184(1-3), 164 -169.

[7] Machado, F.M., Bergmann, C.P., Fernandes, T.H.M., Lima, E.C., Royer, B., Calvete, T., Fagan, S.B. (2011) Adsorption of Reactive Red M-2BE dye from water solutions by multi-walled carbon nanotubes and activated carbon. J. Hazard. Mater. 192(3), 1122-1131.

[8] Sathishkumar, P., Arulkumar, M., Palvannan, T. (2012) Utilization of agro-industrial waste Jatropha curcas pods as an activated carbon for the adsorption of reactive dye Remazol Brilliant Blue R (RBBR). Journal of Cleaner Production, 22(1), 67-75.

[9] Xue, A., Zhou, S., Zhao, Y., Lu, X., Han, P. (2010) Adsorption of reactive dyes from aqueous solution by silylated palygorskite, Appl. Clay Sci. 48, 638–640.

[10] Li, Q., Yuea, Q.-Y., Suc, Y., Gaoa, C., Sun, H.-J. (2010) Equilibrium, thermodynamics and process design to minimize adsorbent amount for the adsorption of acid dyes onto cationic polymer-loaded bentonite. Chem. Eng. J. 158, 489–497.

[11] Tanyildizi, M. Ş. (2011) Modelling of adsorption isotherms and kinetics of reactive dye from aqueous solution by peanut hull. Chem. Eng. J. 168, 1234–1240.

[12] Gil, A., Assis, F.C.C., Albeniz, S., Korili, S.A. (2011) Removal of dyes from wastewaters by adsorption on pillared clays. Chem. Eng. J. 168, 1032–1040.

[13] Errais, E., Duplay, J., Darragi, F., M'Rabet, I., Aubert, A., Huber, F., Morvan, G. (2011) Efficient anionic dye adsorption on natural untreated clay: Kinetic study and thermodynamic parameters. Desalination, 275, 74–81.

[14] Ip, A.W.M., Barford, J.P., McKay, G. (2009) Reactive Black dye adsorption/desorption onto different adsorbents: Effect of salt, surface chemistry, pore size and surface area. J. Colloid Interface Sci. 337, 32–38.

[15] Shen, D., Fan, J., Zhou, W., Gao, B., Yue, Q., Kang, Q. (2009) Adsorption kinetics and isotherm of anionic dyes onto organo-bentonite from single and multisolute systems. J. Hazard. Mater. 172, 99–107.

[16] Qin, Q., Ma, J., Liu, K. (2009) Adsorption of anionic dyes on ammonium-functionalized MCM-41. J. Hazard. Mater. 162, 133–139.

[17] El Boujaady, H., El Rhilassi, A., Bennani-Ziatni, M., El Hamri, R., Taitai, A., Lacout, J.L. (2011) Removal of textile dye by adsorption on synthetic calcium phosphate. Desalination, 275, 10–16.

[18] Leechart, P., Nakbanpote, W., Thiravetyan, P. (2009) Application of 'waste' wood-shaving bottom ash for adsorption of azo reactive dye. J. Environ. Manage. 90, 912–920.

[19] Bingol, D., Tekin, N., Alkan, M. (2010) Brilliant Yellow dye adsorption onto sepiolite using a full factorial design. Appl. Clay Sci. 50, 315–321.

[20] Mahmoodi, N.M., Hayati, B., Arami, M., Lan, C. (2011) Adsorption of textile dyes on Pine Cone from colored wastewater: Kinetic, equilibrium and thermodynamic studies. Desalination, 268, 117–125.

[21] Valix, M., Cheung, W.H., McKay, G. (2004) Preparation of activated carbon using low temperature carbonisation and physical activation of high ash raw bagasse for acid dye adsorption. Chemosphere, 56, 493–501.

[22] Dávila-Jiménez, M.M., Elizalde-González, M.P., Hernández-Montoya, V. (2009) Performance of mango seed adsorbents in the adsorption of anthraquinone and azo acid dyes in single and binary aqueous solutions. J. Biores. Technol. 100, 6199–6206.

[23] Arami, M., Limaee, N.Y., Mahmoodi, N.M., Tabrizi, N.S. (2006) Equilibrium and kinetics studies for the adsorption of direct and acid dyes from aqueous solution by soy meal hull. J. Hazard. Mater. 135, 171–179.

[24] Tsai, W.T., Chang, C.Y., Lin, M.C., Chien, S.F., Sun, H.F., Hsieh, M.F. (2001) Adsorption of acid dye onto activated carbons prepared fromagricultural waste bagasse by $ZnCl_2$ activation. Chemosphere, 45, 51–58.

[25] Mui, E.L.K., Cheung, W.H., Valix, M., McKay, G. (2010) Dye adsorption onto char from bamboo. J. Hazard. Mater. 177, 1001–1005.

[26] Ahlrichs, J.L., Serna, J.C., Serratosa, J.M. (1975) Structural hydroxyls in sepiolite. Clays Clay Miner. 23, 119–124.

[27] Rytwo, G., Tropp, D., Serban, C. (2002) Adsorption and interactions of diquat, paraquat and methyl green on sepiolite. Appl. Clay Sci. 20, 273–282.

[28] Grim, R.E. (1968) Clay Minerology. Second ed., McGraw-Hill, New York.

[29] Frost, R.L., Ding, Z. (2003) Controlled rate thermal analysis and differential scanning calorimetry of sepiolites and palygorskites, Thermochim. Acta, 397, 119–128.

[30] Montgomery, D.G. (2005) Design and Analysis of Experiments. 6th edn, John Wiley Sons, Inc., Arizona, USA.

[31] Imandi, S.B., Bandaru, V.V.R., Sumalanka, S.R., Bandru, S. R., Garapti, H.R. (2008) Application of statistical experimental designs for the optimization of medium constituents for the production of citric acid from pineapple waste. Bioresour. Technol. 99, 4445–4450.

[32] Khalili, Z. and Bonakdarpour, B. (2010) Statistical optimization of anaerobic biological processes for dye treatment. Clean – Soil, Air, Water, 38 (10), 942–950.

[33] Khataee, A.R., Dehghan, G., Ebadi, E., Pourhassan, M. (2010) Central composite design optimization of biological dye removal in the presence of macroalgae *chara sp.* Clean – Soil, Air, Water, 38 (8), 750–757.

[34] Das, D. and Das, N. (2011) Response surface approach for the bisorption of Ag(I) by macrofungus *pleurotus platypus*, Clean – Soil, Air, Water, 39 (2), 157–161.

[35] Turan, N.G., Elevli, S., Mesci, B. (2011) Adsorption of copper and zinc ions on illite: Determination of the optimal conditions by the statistical design of experiments, Appl. Clay Sci. 52, 392–399

[36] Alidokht, L., Khataee, A.R., Reyhanitabar, A., Oustan, S. (2011) Cr(VI) Immobilization process in a Cr-Spiked soil by zerovalent iron nanoparticles: Optimization using response surface methodology, Clean – Soil, Air, Water, 39 (7), 633–640.

[37] Zolgharnein, J., Asanjarani, N., Mousavi, S.N. (2010) Optimization and characterization of Tl(I) adsorption onto modified ulmus carpinifolia tree leaves, Clean – Soil, Air, Water, 39 (3), 250–258.

[38] Rao, K.S., Anand, S., Rout, K., Venkateswarlu, P. (2012) Response surface optimization for removal of cadmium from aqueous solution by waste agricultural biosorbent *psidium guvajava* L. leaf powder, Clean – Soil, Air, Water, 40 (1), 80-86.

[39] Tarangini, K., Kumar, A., Satpathy, G.R., Sangal, V.K. (2009) Statistical optimization of process parameters for Cr (VI) biosorption onto mixed cultures of *Pseudomonas aeruginosa* and *Bacillus subtilis*. Clean, 37(4–5), 319 – 327.

[40] Khataee, A.R., Zarei, M., Khataee, A.R. (2011) Electrochemical treatment of dye solution by oxalate catalyzed photoelectro-fenton process using a carbon nanotube-PTFE cathode: Optimization by central composite design. Clean – Soil, Air, Water, 39 (5), 482–490.

[41] Alkan, M., Demirbas, O., Dogan, M. (2007) Adsorption kinetics and thermodynamics of an anionic dye onto sepiolite. Microporous Mesoporous Mater. 101, 388-396.

[42] Lundstedt, T., Seifert, E., Abramo, L., Thelin, B., Nyström, A., Pettersen, J., Bergman, R. (1998) Experimental design and optimization. Chemom. Intell. Lab. Syst. 42, 3–40.

[43] Palanikumar, K., Dawim, J.P. (2009) Assessment of some factors influencing tool wear on the machining of glass fibre-reinforced plastics by coated cemented carbide tools, J. Mater. Process. Technol. 209, 511–519.

[44] Alkan, M., Demirbas, O. and Dogan, M. (2005) Electrokinetic properties of sepiolite suspensions in different electrolyte media. J. Colloid Interface Sci. 281, 240–248.

[45] Alkan, M., Demirbas, O., Celikcapa, S. and Dogan, M. (2004) Sorption of acid red 57 from aqueous solution onto sepiolite. J. Hazard. Mater. 116, 135–145.

[46] Alkan, M., Demirbas, O., Celikcapa, S. and Dogan, M. (2005) Removal of reactive blue 221 and acid blue 62 anionic dyes from aqueous solutions by sepiolite. Dyes Pigm. 65, 251–259.

[47] Mathialagan, T., Viraraghavan, T. (2005) Biosorption of pentachlorophenol by fungal biomass from aqueous solutions: a factorial design analysis, Environ. Technol. 6, 571–579.

[48] Cojocaru, C., Trznadel, G.Z. (2007) Response surface modeling and optimization of copper removal from aqua solutions using polymer assisted ultrafiltration. J. Membr. Sci. 298, 56–70.

Received: February 25, 2013
Accepted: April 30, 2013

CORRESPONDING AUTHOR

Özkan Demirbaş
University of Balikesir
Faculty of Science and Literature
Department of Chemistry
10145 Balikesir
TURKEY

Phone: +90(266)6121000
Fax: +90(266)6121215
E-mail: ozkan@balikesir.edu.tr

FEB/ Vol 22/ No 12/ 2013 – pages 3501 – 3510

THE INFLUENCE OF WATER OSCILLATION ON THE VERTICAL DISTRIBUTION OF *MICROCYSTIS* COLONIES OF DIFFERENT SIZES